ELSEVIER

Journal of Alloys and Compounds 317–318 (2001) 411–418

Journal of ALLOYS AND COMPOUNDS

www.elsevier.com/locate/jallcom

Structural characterisation and corrosion resistance of Ga-precious metal alloys formed by liquid–solid reaction at room temperature

M.R. Pinasco[a,*], E. Angelini[b,1], E. Cordano[a], F. Rosalbino[b]

[a]*Chemistry and Industrial Chemistry Department, University of Genoa, Via Dodecaneso 31, 16146 Genoa, Italy*
[b]*Material Science and Chemical Engineering Department, Polytechnic of Turin, Corso Duca degli Abruzzi 24, 10129 Turin, Italy*

Abstract

An attempt to eliminate Hg from dental amalgams was made by substituting it with low melting Ga-based alloys, liquid at room temperature. However more information is needed on the influence of alloy composition and their questioned corrosion resistance. In this paper the reaction of some liquid Ga alloys and some solid precious metal alloys with different nobility was studied. Structural features, hardness and corrosion resistance of the obtained composite materials were investigated as a function of composition of the starting alloys, liquid/solid ratio and different mixing methods. Every combination of the solid precious metal powders and the liquid Ga-alloys gives rise to similar composite materials. The structure always consists of unreacted solid alloy particles embedded in a complex matrix composed of many reaction phases. The formation of some phases depends on the composition of the solid alloy, others originate all the time; however their topography and morphology may be different as well as their compositional range. The high porosity generally present in the composite materials markedly affects hardness values; nevertheless some prepared materials reach hardness comparable with the one of commercial amalgams. The nobility of the solid alloy and porosity percentage play a determinant role on the corrosion behaviour. In all cases the low corrosion resistance of the experimented materials may be attributed to a galvanic coupling between the reaction intermediate phases and the unreacted liquid alloy remained inside the pores.

Keywords: Intermetallics; Dental alloys; Electrochemical reactions; Metallography

1. Introduction

The controversies concerning the use of mercury in dental amalgams led to the research of alternative materials for restorative odontology [1–3]. However because of its low cost, rapidity and easy application as well as its suitable mechanical properties, this material continues to be used especially in social dentistry. An attempt to eliminate Hg from dental amalgams was made by substituting it with low melting Ga-based alloys, liquid at room temperature [4,5]. Some gallium alloys are present on the Japanese and Australian markets [6]: alloy powders with compositions similar to those for amalgam alloys are triturated with a liquid gallium alloy. The mix can be condensed into a prepared cavity in the same way as for amalgam. Some properties (compressive and tensile strength, hardness, creep, wear resistance) resulted in being similar to those of leading high copper amalgams. Gallium may decrease environmental risks since its vapour pressure is lower than mercury [7] and it has been found to be less cytotoxic [8]. However in vitro and in vivo studies have expressed concern in relation to the corrosion resistance of Ga alloys [9,10]. To improve the corrosion resistance of this kind of alloy, it is worth studying the phases formed by the reaction between some liquid Ga alloy formulations and solid alloys containing precious metals.

Our research deals with the investigation and the characterisation of the phases originated by the reaction of liquid Ga alloys based on the system Ga–In–Sn and some Au based and Ag based solid alloys. Moreover the corrosion resistance of the metal composite products obtained was evaluated.

2. Experimental details

By means of the analysis of the literature and of the available equilibrium diagrams [11,12], three alloys, liquid at room temperature, were selected and produced; the compositional range (wt.%) of the constituent elements was: $62<Ga<65.6$, $19<In<25$ and $13<Sn<16$; other

*Corresponding author. Fax: +39-10-362-5051.
E-mail addresses: metal@chimica.unige.it (M.R. Pinasco), angelini@polito.it (E. Angelini).
[1]Fax number: +39-011-564-4699.

0925-8388/01/$ – see front matter
PII: S0925-8388(00)01418-3

minor elements were added. These three alloys were mixed with two precious metal alloy powders of different nobility, whose principal elements were Au (alloy A, high nobility) and Ag (alloy B, low nobility), in two ratios: liquid:solid=1:1 and 0.65:1, with two different mixing methods: manual and with a dental vibrator. The solid alloys were powdered with mechanical methods obtaining irregular needle-like particles, with dimensions variable up to 200 μm in length.

The obtained materials after liquid–solid reaction were characterised, 1 week after preparation, by optical and electron microscopy (SEM–SE and BSE), EDS microanalysis, image analysis, X-ray diffraction (radiation: Co Kα, diffraction angle 2θ range: 10–120°), and hardness measurements (HV_1). Their corrosion behaviour was evaluated by means of potentiodynamic anodic polarization curves performed at room temperature in aerated synthetic saliva (KH_2PO_4 0.26 g; $NaHCO_3$ 1.50 g, KSCN 0.33 g, Na_2HPO_4 0.19 g; NaCl 0.70 g; Urea 0.13 g; distilled water up to 1 dm^3). The curves were recorded starting from the free corrosion potential, at a scan rate $dE/dt=0.25$ mV/s. A saturated calomel electrode (SCE) was used as reference electrode. The surface of all samples was reexamined by SEM after the electrochemical tests in order to investigate the corrosive attack features.

3. Results and discussion

3.1. Structural characterisation

For every combination of solid precious metal powders and Ga liquid alloy the reaction generated a particle reinforced composite material: the unreacted solid alloy particles are embedded in a matrix which is composed of new developed reaction intermediate phases. Figs. 1 and 2 show the microstructure of two materials obtained mixing in ratio 0.65:1, in the vibrator, alloy A (code MAT A 0.65v) and alloy B (code MAT B 0.65v) powders with the same liquid alloy, with a Ga content of 62 wt.%. It is evident that some of the powder particles remain unreacted; their sizes are smaller in the material obtained from alloy B. The starting dimensions of the solid alloy A particles were a little larger, but the resulted fineness of the structure of MAT B 0.65v and the smaller size of the unreacted alloy B are probably a consequence of its higher reactivity, also demonstrated by the rounded morphology of the remaining particles and by the shorter hardening time of the relative metal mixture. As a matter of fact the reaction zone of MAT B was always wider.

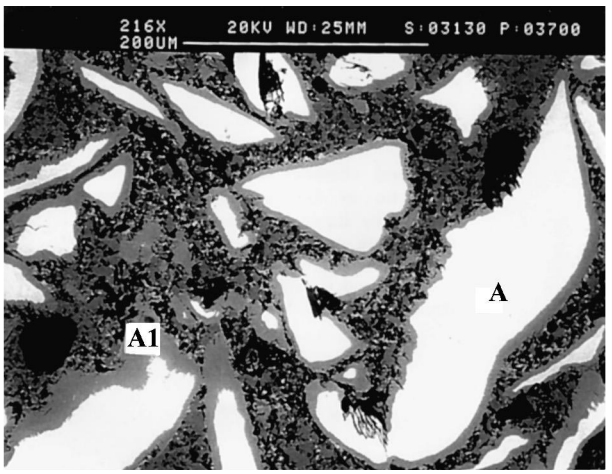

Fig. 1. (SEM–BSE). MAT A 0.65v: general features of the structure: unreacted solid alloy particles (A) embedded in a polyphasic reaction zone.

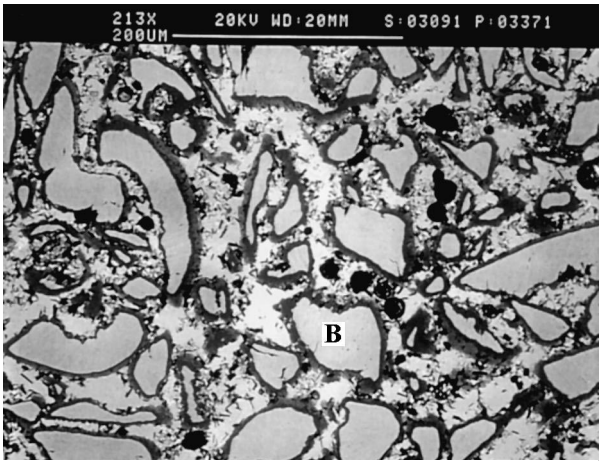

Fig. 2. (SEM–BSE). MAT B 0.65v: general view of the structure with remaining rounded solid alloy particles (B) and intermediate phases in the reaction zone.

The complex multiphase reaction zone is particularly evidenced by SEM–BSE examination for the marked compositional differences among the new formed phases. The composition of the various phases (as measured by X-ray energy dispersive spectroscopy) found in the composite material MAT A 0.65v, shown in Fig. 1, is listed in Table 1.

The remaining solid alloy particles (A) of alloy A are surrounded by a light grey phase (phase A1), containing mainly Au and Ga with small additions of Cu and Pt (Fig. 1). The contiguous reaction zone connecting the unreacted particles includes several randomly distributed phases, both of different grey tonalities and completely dark (Fig. 3). The dark phase (phase A2), in the shape of either irregular or polygonal grains or rods spread in the matrix, contains Ga (as main element) together with Cu. This phase resulted principally binary, however small additions of other metals, such as Au and In, could be present. The matrix of the reaction zone (phase A3), which is greyer than phase A1, extends either in wide or limited zones among the other phases (Fig. 3); it contains Ag, Sn and In and small amounts of Ga and Cu of less than 1 wt.%.

Table 1
Composition of the phases evidenced in the materials MAT A 0.65v and MAT B 0.65v (liquid:solid alloys ratio=0.65, mixed in the vibrator)[a]

Material	Phase	Main elements	Compositional range (wt.%)								
			Ga	In	Sn	Au	Ag	Cu	Pd	Pt	Others
MAT A	A1	Au, Ga	38–40	–	–	51–52	–	2–3	–	5–6	–
0.65 v	A2	Ga, Cu	63–66	1–3	–	1–3	–	31–33	–	–	–
	A3	In, Ag	<1	59–62	4–6	–	32–33	<1	–	2–3	X
	A4	Au, In	2–8	45–51	–	38–39	1–4	1–3	–	–	X
	A5	Sn, In	7–8	20–21	64–65	4–5	–	2–3	–	–	–
MAT B	B1	Pd, Ga	74–75	–	–	–	–	1–2	23–24	–	X
0.65 v	B2	Ga, Cu	65–66	–	–	–	X	31–32	1	–	–
	B3	In, Ag	<1	61–62	4–5	–	33–34	–	–	–	–
	biphasic zone		61–62	3–4	14–15	–	–	<1	18–19	–	X
	B4	Au, Ga	38–39	3–4	X	53–54	–	1–2	–	–	–
	B5	Sn, In	1–2	19–20	77–78	–	X	–	–	–	–
	B6	Ag, In	1–3	30–31		65–67	–	–	–	–	–
	B7	Au, In	4–10	34–40	2–6	45–56	X	X	X	–	–

[a] X=element sometimes present in small percentages.

Islands of phase A1 and irregular shaped particles of phase A4, bright white in colour and very small in size, may be observed dispersed in the matrix; the latter mainly contains In and Au with few percentages of other elements. Another phase (phase A5), light grey in colour and with irregular boundaries, contained Sn, In and little Ga. It could derive from the remains of the liquid alloy, solidified after its compositional change caused by the reaction itself.

In the material MAT B 0.65v obtained from the reaction of alloy B with the same liquid alloy (Fig. 2) most of the detected phases were analogous to those identified in MAT A 0.65v. Their composition is listed in Table 1. The phase (phase B1) surrounding the unreacted solid particles (B) is here composed of Pd and Ga, Ga being the main element. The brighter wider zones, constituting the reaction zone matrix, principally contain Ag and In alternatively predominant in ratio of about 2:1 (phase B6 and B3), with a small Ga content (Fig. 4). In MAT A 0.65v, previously described, only the phase with a higher In amount (phase A3) was detected, probably due to the less Ag content in the solid alloy. Hero et al. [13] found the Ag_9In_4 phase with similar composition in the studied Ga alloy LU; the same phase Ag_9In_4 in the commercial Ga alloy GF [5,13] contains Pd and a minor amount of In and Ag. Although solid alloy B is richer in Pd than GF powders [13], phase B6 does not contain Pd, the latter being mainly involved in the formation of the phase B1 (with Pd and Ga) surrounding the remaining solid alloy. At the boundaries of phase B1, lamellar or globular biphasic zones ('biphasic zone', BF) are present (Fig. 4); their mean composition seems to suggest that these structural aspects are a very fine mixture of the phases with Ga–Pd and Ag–In. A phase with Ga and Cu (phase B2) identical in morphology and composition (except the minor elements) to the one of MAT A 0.65v (phase A2) was observed. Such a kind of phase was

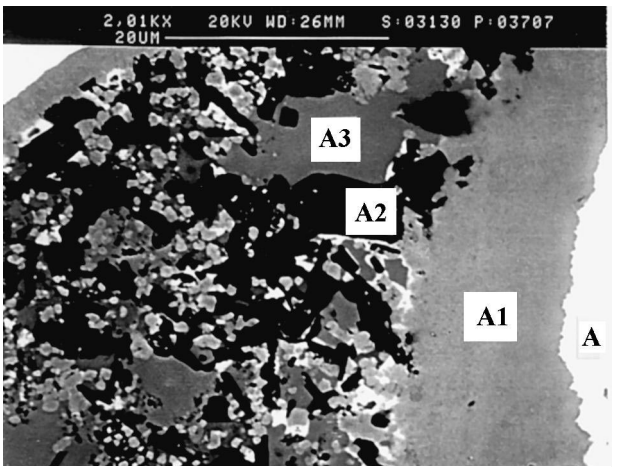

Fig. 3. (SEM–BSE). MAT A 0.65v: reaction zone between two remained particles of alloy A appearing white. Several intermediate phases different in colour are visible.

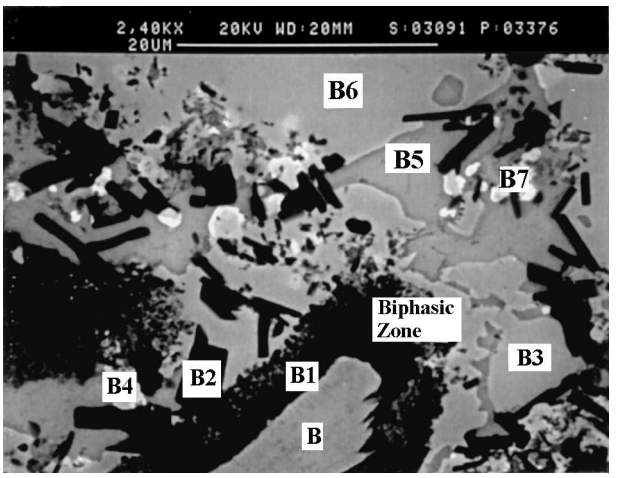

Fig. 4. (SEM–BSE). MAT B 0.65v: intermediate phases in the reaction zone with a remained alloy B particle.

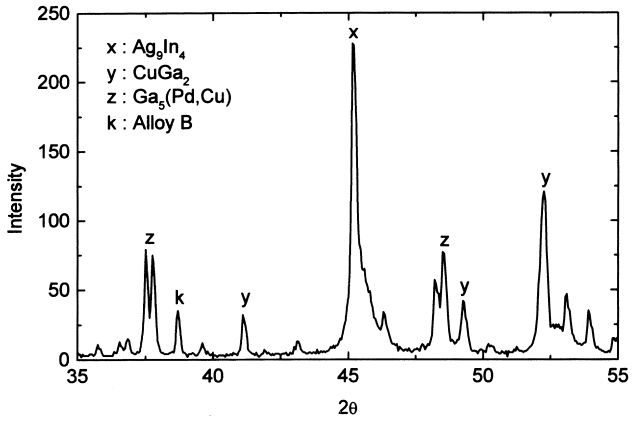

Fig. 5. Selected region of X-ray diffractogram of MAT B 0.65v.

also shown in commercial alloys deriving from Ga liquid alloys and solid alloys with Ag and Cu [5,6,13]; but this phase in these latter materials has a different topography surrounding the unreacted spherical particles. A bright Au-Ga based phase (phase B4) was found, having a morphology similar to that of the phase A4 in MAT A 0.65v, where In is associated to Au, but its composition is about the same as that of phase A1. Owing to the less Au amount in the solid alloy this phase becomes a minority. Moreover very small grains (phase B7) appearing white and very bright are scattered in the reaction zone; they contain mainly Au and In where Ga is a minority. However EDS microanalysis revealed a wide compositional range, in fact the size of this phase is too small and the relative EDS results might suffer the signals of the other embedding phases. Finally another phase (phase B5) was observed in the microstructure, appearing grey and distinguishable owing to the relief differences with respect to the other phases (Fig. 4). It contains the metals of the liquid alloy: Sn, as the main element, In and a little Ga. Compared to the corresponding phase detected in MAT A 0.65v (phase A5), a higher Sn amount and a lower Ga content, largely consumed in the formation of phase B1, are present. A phase containing the same elements and with a similar feature was also identified in literature regarding Ga alloys GF and LU [5,13]; its composition however is different, varying especially in In content.

X-ray diffraction analysis was performed on both MAT A and MAT B mixed in the vibrator in liquid/solid ratio 0.65. Only a few phases visible in the microstructure were clearly identified. Fig. 5 shows a part of the X-ray diffraction pattern of MAT B 0.65v, where three main phases deriving from the reaction between the solid powders and the liquid alloy are shown: phase B1 (*z*), phase B2 (*y*) and phase B6 (*x*). On the basis of JCPDS index cards [14] and the composition determined by EDS microanalysis, these phases were identified as the cubic Ag_9In_4 ($a=0.9922$ nm), the tetragonal $CuGa_2$ ($a=0.2830$ nm and $c=0.5839$ nm) and the tetragonal Ga_5(Pd,Cu) ($a=0.6455$ nm and $c=1.0010$ nm). Moreover the main cubic face-centred phase (*k*) of the unreacted solid alloy B was also detected. Other peaks present in the X-ray patterns could not be attributed to any phase, although characterised by microscopy and EDS microanalysis. The phases Ag_9In_4 and $CuGa_2$ together with the cubic face-centred phase of solid alloy A were also evidenced in the X-ray diffraction patterns of MAT A. Our experimental data and those found in literature [5,13] reveal that the two intermediate phases Ag_9In_4 and $CuGa_2$ always originated, even if the reacting solid alloys have remarkable differences in composition; nevertheless their topography and morphology were not the same.

Considering the influence of the preparation method on the structure of the metal composite material with the same liquid/solid alloy ratio, it is possible to observe that the general feature of the microstructure is analogous. However in the material mixed with the vibrator the reaction zone is more extensive, the phases are better defined with sharper boundaries and they have a more regular distribution. A lower presence of the minor elements was detected in every phase, with the phase composition becoming binary or ternary (see Table 1 vs. Table 2). The highest variations occur in the phases containing Au.

Table 2
Composition of the phases evidenced in the material MAT B 0.65 m (liquid:solid alloys ratio=0.65, manual mixing)[a]

Material	Phase	Main elements	Compositional range (wt.%)								
			Ga	In	Sn	Au	Ag	Cu	Pd	Pt	Others
MAT B	B1	Pd, Ga	71–72	X	–	X	X	2–7	19–23	–	X
0.65 m	B2	Ga, Cu	60–64	1–5	X	X	X	24–31	1–2	–	–
	B3	In, Ag	<1	58–61	4–8	–	33–34	–	–	–	–
	biphasic zone		58–63	4–8	–	X	6–15	1–2	17–19	–	–
	B4	Au, Ga	29–37	11–19	2–5	43–51	–	2–3	–	–	X
	B5	Sn, In	1–2	19–21	73–79	–	X	–	–	–	–
	B6	Ag, In	1–2	28–32	–	–	60–67	0–2	–	–	X
	B7	Au, In	2–4	3–13	4–6	72–90	X	2–4	X	–	–

[a] X=element sometimes present in small percentages.

Despite the difficulties related to the small size of these phases, EDS microanalysis make it possible to highlight a marked change in the mean composition, as shown by the comparison between Tables 1 and 2. The decrease in Au and the increase in In are particularly evident in Au-In based phase B7 prepared by means of the vibrator. Moreover a quantitative re-distribution of the various phases occurred. An evident example could be noted in MAT B, where the phase around the unreacted powders has a quite higher thickness in the vibrator mixed material and the phase B7 is noticeably reduced in its quantity.

Regarding the influence of liquid:solid ratio, mixing the liquid and the solid alloys in ratio 1:1 gives rise to a microstructure similar to that of the respective materials in ratio 0.65. Phases are present with analogous morphology and distribution in the reaction zone; the ratio between the extension of the reaction zone and the residual solid alloy becomes higher passing from the liquid:solid ratio 0.65 to 1, where mixing is manual. If the mixing is carried out in a vibrator, differences are less evident: as a matter of fact, the mixing in the vibrator modifies in the same way but more effectively than the increase of liquid:solid ratio, extending the reaction zone. Concerning the phase composition, EDS microanalysis on the single phases generally did not reveal marked differences, except for the phase B7 Au–In in MAT B (Table 3). Moreover the upper limit of Ga compositional range generally seems to increase.

The global mean composition of the obtained materials is modified by the experimental parameters (ratio and mixing method) only concerning Ga, In and Sn contents, as Fig. 6 shows.

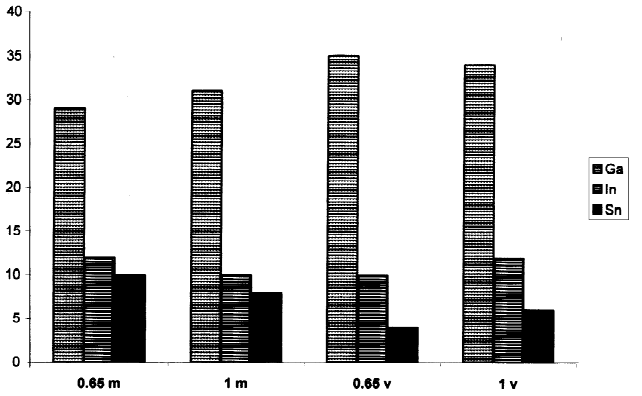

Fig. 6. Amount (wt.%) of Ga, In and Sn in the mean composition of MAT B as a function of the preparation parameters.

3.2. Porosity

In every examined material high porosity percentages were evidenced, with pores irregular in shape and variable in size (Fig. 2). Unreacted liquid Ga-alloy is trapped in these pores and rest in the hardened material. Fig. 7 shows the results of MAT B achieved by means of image analysis as a function of the considered experimental parameters. The porosity is about halved by mixing the alloys in the vibrator, although it still remained high. The different liquid–solid alloy ratio affects porosity less than the mixing method.

A similar trend was evidenced in MAT A, however its porosity values were generally higher than in MAT B.

3.3. Hardness

Fig. 8 shows HV_1 hardness values of MAT A and MAT B in relation to the used experimental parameters. Some commercial Hg-amalgam hardness values for comparison are also reported. By examining the effect of the various parameters on the hardness values of MAT A and MAT B, it can be observed that the influence of the liquid:solid ratio is hardly noticeable and seemingly contradictory, while passing from the manual method to the mixing with the vibrator leads to an increase in hardness, reaching values comparable with the ones of commercial Hg dental amalgams. The comparison between Figs. 7 and 8 shows that the hardness values strictly depend on the porosity

Table 3
Composition of the phases evidenced in the material MAT B 1 m (liquid:solid alloys ratio=1, manual mixing)[a]

Material	Phase	Main elements	Compositional range (wt.%)								
			Ga	In	Sn	Au	Ag	Cu	Pd	Pt	Others
MAT B	B1	Pd, Ga	67–74	X	–	X	X	2–5	19–23	–	X
1 m	B2	Ga, Cu	58–67	1–6	X	X	X	24–31	1–2	–	–
	B3	In, Ag	<1	58–61	4–8	–	33–34	–	–	–	–
	biphasic zone		58–63	3–8	–	–	7–15	–	17–19	–	–
	B4	Au, Ga	22–45	12–23	X	44–54	X	1–4	X	–	–
	B5	Sn, In	1–4	19–22	69–78	–	X	–	–	–	–
	B6	Ag, In	1–2	30–32	–	–	65–67	–	–	–	X
	B7	Au, In	3–15	36–46	2–14	37–44	X	1	X	–	–

[a] X=element sometimes present in small percentages.

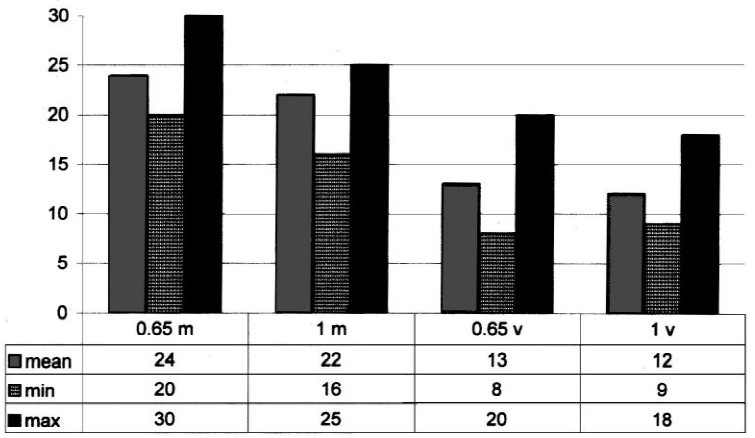

	0.65 m	1 m	0.65 v	1 v
mean	24	22	13	12
min	20	16	8	9
max	30	25	20	18

Fig. 7. Porosity percentage of MAT B in relation to the different preparation parameters.

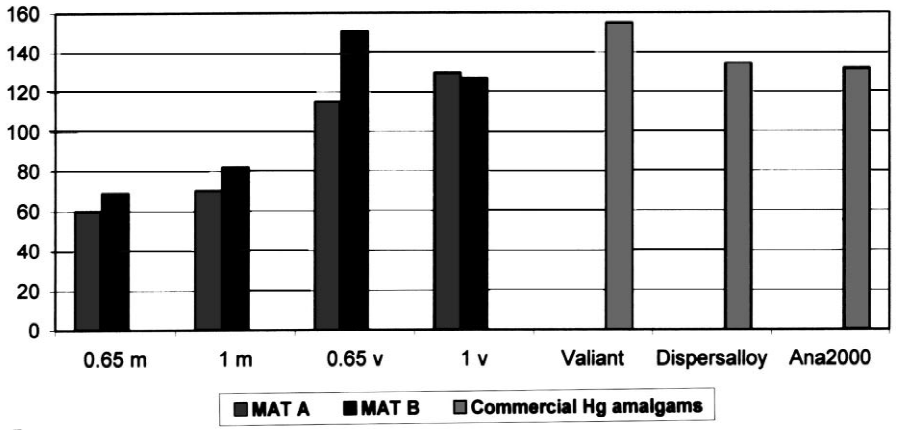

Fig. 8. HV_1 hardness values of MAT A and MAT B in relation to the used experimental parameters in comparison to the hardness values of some commercial Hg-amalgams.

degree: a higher hardness value corresponds to a less porosity degree, independently of the liquid:solid ratio.

3.4. Electrochemical characterisation

The nobility degree of the solid alloy and the porosity percentage, influenced by the mixing parameters, play a determinant role on the corrosion behaviour of the experimented materials. In all cases the low corrosion resistance exhibited by these materials may be attributed to a galvanic coupling between the reaction intermediate phases and the unreacted liquid alloy remained inside the pores. The formation of this galvanic short-circuit cell [15] is responsible for the high anodic current densities observed in potentiodynamic tests, particularly in the potential range of interest in the oral cavity, −100 to +300 mV (SCE) [16].

The effect of the different nobility degree of solid alloy is shown in Fig. 9, where the anodic polarisation curves recorded in synthetic saliva for MAT A 0.65v and MAT B 0.65v are reported. In both cases the abrupt increase of current density may be attributed to the onset of galvanic corrosion where the unreacted liquid alloy acts as anode of the short-circuit cell.

As a matter of fact, during the corrosion test the

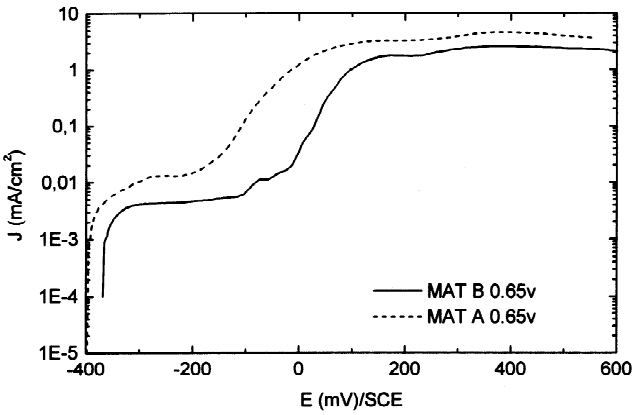

Fig. 9. Anodic polarisation curves recorded in aerated synthetic saliva for MAT A 0.65v and MAT B 0.65v.

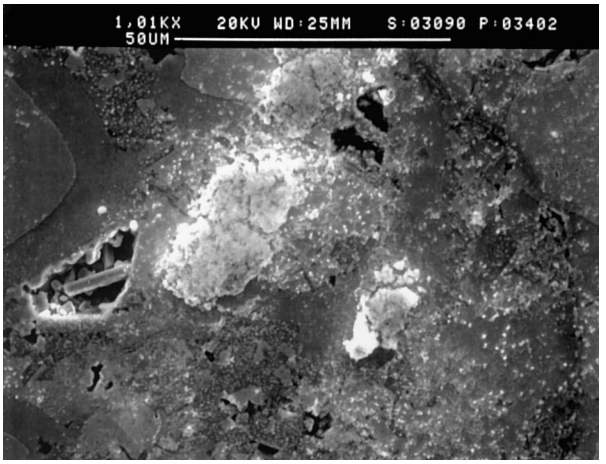

Fig. 10. (SEM–SE). MAT B 1v after the electrochemical test in aerated synthetic saliva deposits on the surface.

discharge of a colloidal white product from the exposed samples' surface was observed by eye and it may be GaO(OH) as referred in literature regarding commercial Ga alloys [6]. By means of SEM–SE observation of the surface samples after the electrochemical tests, there is only slight evidence of the reaction zone. Only in some zones of the samples always associated to high porosity, can corrosion products be observed of different colour and nature (Fig. 10). Some of them, appearing lighter to SEM–SE observation, are mainly constituted by Sn as prevalent element (55–67 wt.%), In in low amount (3–4 wt.%), little Ga content (1<Ga<3 wt.%), Cl (7–9 wt.%) and S in trace. Others, grey in colour, contain principally In (22–26 wt.%), Sn (19–23 wt.%) and Ga (4–11 wt.%) with Cl (5–6 wt.%) and P (about 4 wt.%). Oxygen may also be present. Generally the corrosive process originated the formation of thin deposits like a little dot (Fig. 11), preferentially localised on Ag–In and Ga–Cu phases. The comparison of the global analysis of the surface of MAT B

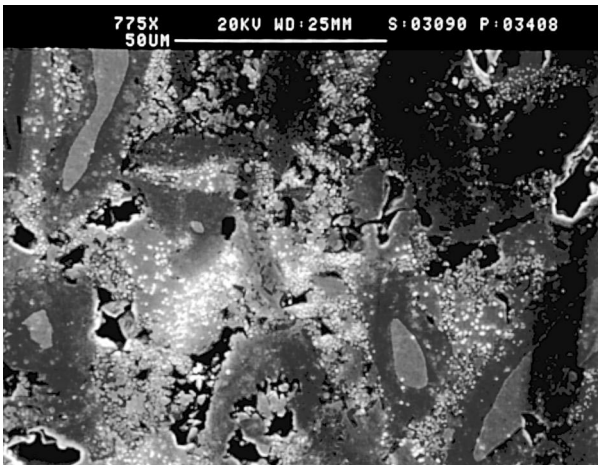

Fig. 11. (SEM–SE). General view of the surface of MAT B 1v after the electrochemical test in aerated synthetic saliva.

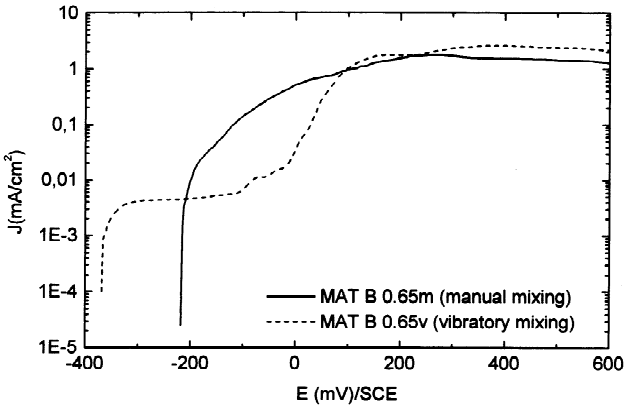

Fig. 12. Anodic polarisation curves recorded in aerated synthetic saliva for MAT B obtained by two different mixing methods.

0.65 and MAT B 1 before and after the electrochemical test revealed an increase in Sn content and a slight decrease in Ga amount. Considering all the obtained experimental results they agree with the possibility of the dissolution of the liquid alloy trapped in the porosity and its possible partial re-deposition as low soluble products containing mainly Sn, In and Cl and, may be, oxygen.

Considering Fig. 9, again one can observe that MAT A exhibits higher anodic current densities and the onset of galvanic corrosion is shifted towards more negative potentials. This behaviour may be attributed (the sample porosity is similar) to an accentuated galvanic corrosion phenomenon due to the presence of unreacted liquid alloy and reaction intermediate phases with higher nobility (Table 1).

The influence of the porosity degree on corrosion behaviour of the tested metal composite materials is well-evidenced in Fig. 12, which shows the anodic polarisation curves recorded in synthetic saliva for the MAT B obtained by two different mixing methods. As previously stated, manual mixing leads to the formation of a material with higher porosity percentage (Fig. 7). The higher porosity degree is responsible for the rapid increase of anodic current density observed in this case (Fig. 12), as a consequence of an accentuated galvanic short-circuit cells phenomenon [15].

4. Conclusions

- Every combination of the solid precious metal powders and the liquid Ga-alloys gives rise to similar composite materials. The structure always consists of unreacted solid alloy particles embedded in a complex matrix composed of many reaction intermediate phases.
- Some phases result in relation to the composition of the solid alloy, others ($CuGa_2$, Ag_9In_4 and the Sn–Ga–In phases) originate all the time; however their topography

and morphology may be different as well as their compositional range.

- The liquid:solid ratio and the mixing method have some influence on the composition, distribution and quantity of the reaction phases as well as on the extent of the whole reaction zone.
- The mean composition of the composite material is affected by the experimented parameters mainly in relation to Ga, Sn and In content.
- The high porosity generally present in the composite materials is reduced by mixing the mixture in a vibrator. It markedly affects the hardness values; nevertheless some prepared materials reach hardness comparable with the one of commercial amalgams.
- The nobility of the solid alloy and the porosity percentage play a determinant role on the corrosion behaviour. In all cases the low corrosion resistance of the experimented materials may be attributed to a galvanic coupling between the reaction intermediate phases and the unreacted liquid alloy remained inside the pores.

Acknowledgements

This research was financially supported by CNR (PFMSTA II-Sott. Biomaterials). We gratefully thank P.M. Bovone of Puppo Iori and C. for the collaboration and for supplying the metals for this research. In addition the authors are grateful to Miss Gabriella Pellati, for the active work during her degree thesis.

References

[1] J. Dodes, Operat. Dent. 13 (1988) 32.
[2] I. Ahmad, J.G. Standard, Operat. Dent. 15 (1990) 207.
[3] J. Ekstrand, L. Bjorkman, C. Edlund, G. Sandborgh-Englund, Eur. J. Oral Sci. 106 (1998) 678.
[4] T. Horibe, Y. Okamoto, S. Naruse, J. Fukuoka Dent. Coll. 12 (1986) 198.
[5] H. Hero, T. Hokabe, Cells Mater. 4 (1994) 409.
[6] B. Reusch, J. Geis-Gerstorfer, C. Ziegler, Appl. Phys. A 66 (1998) S805.
[7] Y. Oshida, B.K. Moore, Dent. Mater. 9 (1996) 234.
[8] J.E. Chandler, H.H. Messer, G. Ellender, J. Dent. Res. (Abstract number 2109) 72 (1993) 367.
[9] H. Hero, T. Hokabe, H. Wie, J. Mat. Sci.: Mat. Med. 8 (1997) 357.
[10] R. Venugopalan, J.C. Broome, L.C. Lucas, Dent. Mater. 14 (1998) 173.
[11] T.B. Massalski (Ed.), Binary Alloy Phase Diagrams, American Society for Metals, Metals Park, OH 44073, USA, 1990.
[12] G. Petzow, G. Effenberg (Eds.), Ternary Alloys, VCH Publishers, Weinheim, 1995, ISBN 0-89573-847-3
[13] H. Hero, C.J. Simensen, R.B. Jorgensen, Biomaterials 17 (1996) 1321.
[14] JCPDS-ICDD index cards, International Centre for Diffraction Data, 1997.
[15] H. Kaesche, Metallic Corrosion, NACE, Houston, TX, 1985.
[16] J.G. Ewens, E.H. Greneer, J. Oral Rehab. 12 (1985) 469.